NOTES AND CORRESPONDENCE

On Thermal Expansion over the Last Hundred Years

J. R. DE WOLDE, R. BINTANJA, AND J. OERLEMANS

Institute for Marine and Atmospheric Research, Utrecht University, Utrecht, the Netherlands

10 June 1993 and 11 May 1995

ABSTRACT

Estimates of sea level rise during the period 1856–1991 due to thermal expansion are presented. The estimates are based on an ocean model that consists of three zonally averaged ocean basins representing the Atlantic, Pacific, and Indian Oceans. These basins are connected by a circumpolar basin that represents the Southern Ocean. The ocean circulation in the model was prescribed. Surface ocean forcing was calculated from observed sea surface temperatures. Global mean forcing and regionally varying forcing were distinguished. Different parameterizations of ocean heat mixing were incorporated. According to the model presented, global mean sea level rise caused by thermal expansion over the last hundred years ranged from 2.2 to 5.1 cm, a best estimate being 3.5 cm.

1. Introduction

In the past, sea level changes have varied widely on different time and space scales. On longer timescales (ice ages), the global mean sea level varied by more than a hundred meters, but after the latest deglaciation event sea level changes have been considerably smaller. Many different processes affect sea level change. Some of these, for example, isostatic adjustment of the earth's crust, tectonic movements, and river sedimentation, have only regional effects. Others, like melting of large continental ice sheets, smaller ice caps, and glaciers and thermal expansion of sea water are of global interest, although the latter is thought to be of regional importance also (Mikolajewicz et al. 1990). Variability and uncertainties in these processes considerably hamper the determination of recent sea level change. Nevertheless, according to most estimates based on tide-gauge measurements, the global mean sea level rise over the last hundred years was 10–20 cm (Douglas 1991; Woodworth 1993). Melting of glaciers and small ice caps and thermal expansion of sea water are generally thought to be the main contributors to this rise, but there are still uncertainties about their relative importance. Whereas according to Barnett (1985) only a small part of the observed global mean sea level rise is due to thermal expansion, Robin (1986) estimated that one-third of the observed sea level change could be explained by thermal expansion, and Gornitz et al. (1982) even considered that one-half was due to thermal expansion. Both Warrick and Oerlemans (1990) and Wigley and Raper (1993) calculated that thermal expansion and the melting of glaciers and small ice caps were of approximately equal importance for the sea level rise. The contribution made by melting of the Greenland ice sheet was smaller.

Estimates of the contribution made by thermal expansion to the observed sea level rise are hindered by the complex behavior of the density of sea water. Knowledge of the history of the three-dimensional ocean temperature and salinity fields is required for these estimates because the density of sea water is a nonlinear function of pressure, salinity, and temperature. Because of the lack of observations, this knowledge is not available. A general circulation model of the oceans (OGCM) could therefore serve as an important tool to estimate thermal expansion. In a few studies, such models have been used to study future thermal expansion in relation to global warming. Using a prescribed ocean surface forcing, Mikolajewicz et al. (1990) found regional changes in sea level rise due to thermal expansion that are of the same order as the global mean. On the other hand, Church et al. (1991) presented calculations of sea level rise caused by thermal expansion that contain hardly any regional variations. Their ventilated isopycnal ocean model was, as in the present analysis, forced by a prescribed atmospheric temperature change. Cubasch et al. (1992) used a coupled atmosphere–ocean GCM to estimate thermal expansion over the next hundred years. According to their results, the sea level will rise by less than has been

Corresponding author address: J. R. de Wolde, Institute for Marine and Atmospheric Research, Utrecht University, P.O. Box 80.005, 3508 TA Utrecht, the Netherlands.

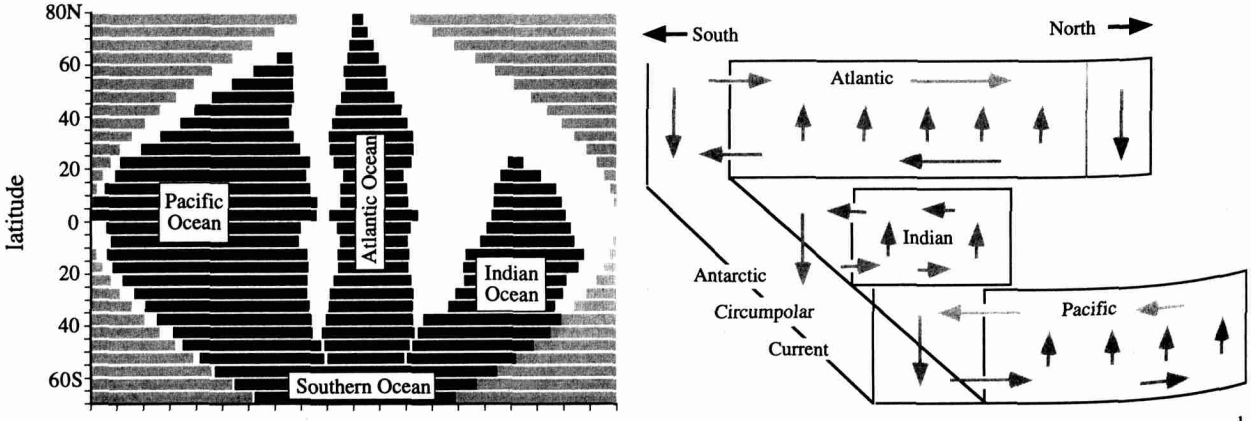

FIG. 1. (a) Geometry of the three zonally averaged ocean basins that are joined at 55°S to form the Southern Ocean. Oceans are represented by black bars and land areas are represented by white bars. The lengths of the black bars represent the ocean basin widths used in the model calculations. Bar centers are chosen so to follow the curvature of the earth: therefore distances between bar centers have no meaning. (b) Schematic review of the ocean circulation pattern. Upwelling and downwelling are represented by vertical arrows and meridional velocities are represented by horizontal arrows.

estimated on the basis of simple upwelling–diffusion models, although they attribute a major part of the difference to the previous warming history prior to the start of the integration. Gregory (1993) studied global and local sea level changes on the basis of a model run of 75 yr, also with a coupled atmosphere–ocean GCM, while Manabe and Stouffer (1994) performed integration of a coupled atmosphere–ocean GCM in order to speculate about future thermal expansion over a period of 500 yr.

However, no simulations of past thermal expansion made on the basis of GCMs have been published. Church et al. (1991) used a three-dimensional ventilated ocean model and estimated that thermal expansion of the oceans between 1900 and 1980 was 5.5 cm. They forced their model by assuming that there was a globally uniform increase in the atmospheric temperature. Nevertheless, most estimates of past thermal expansion are based on simple one-dimensional (upwelling) diffusion models. Gornitz et al. (1982) were the first to estimate thermal expansion of sea water over the past hundred years assuming that the global mean surface air temperature increased by about 0.4°C. They used a one-dimensional ocean model in which ocean mixing is parameterized by diffusion. Because a pure diffusion model leads to an isothermal steady-state ocean temperature profile, Wigley and Raper (1987, 1993) used a one-dimensional upwelling–diffusion energy-balance climate model. In such models global uniform upwelling is assumed to be balanced by high-latitude downwelling, which is a simple representation of the thermohaline circulation. Inclusion of the advective upwelling term ensures more realistic steady-state vertical ocean temperature distributions. Wigley and Raper (1993) tuned their model-calculated radiative forcing so that simulated changes in the global mean air temperature in the past were comparable to observations. They determined that thermal expansion during the period 1880–1990 contributed 2.7–5.6 cm to the observed global mean sea level rise, a best estimate being 3.8 cm.

Because latitudinal variations in ocean temperature are of the same order as vertical variations, it is questionable whether thermal expansion can be correctly simulated with a one-dimensional (vertical) model. Wigley and Raper (1987, 1993) partly dealt with this problem by subdividing their ocean into three zones per hemisphere, each with its own temperature profile and expansion coefficient. In the present paper a different approach is used: a two-dimensional upwelling–diffusion ocean model is used to estimate past thermal expansion. Although in most previous studies the ocean surface was forced by radiation, the ocean forcing in this study is based on observations of sea surface temperatures. We examine the effect on thermal expansion of a global mean forcing type and regionally varying forcing types. In addition, we consider the importance of several parameterizations of the ocean heat mixing. Section 2 describes the ocean model and these parameterizations and section 3 deals with the ocean surface forcing. The results of simulations of the thermal expansion of sea water over the last hundred years are presented in section 4.

2. The thermal expansion model

An idealized ocean model was used for the simulations of the thermal expansion of the oceans. The model consists of three zonally averaged (two-dimensional) ocean basins representing the Atlantic, Pacific, and Indian Oceans. The Atlantic Ocean extends from 55°S to 80°N, the Pacific Ocean from 55°S to 60°N, and the Indian Ocean from 55°S to 20°N. As shown in Fig. 1a, the three basins are connected by a circumpolar basin

(55°S–70°S), which represents the Southern Ocean. The total ocean depth of 4000 m is divided into 10 horizontal layers of increasing thickness with depth, the thickness of the uppermost layer measuring 50 m. Further vertical refinement scarcely affects the results of the model. The horizontal resolution is five meridional degrees. Each ocean basin is assumed to have a fractional zonal width that varies with latitude.

The global thermohaline circulation is prescribed by downwelling in the northern Atlantic (65°–80°N) and in the Southern Ocean basin, which balances uniform upwelling elsewhere. The meridional velocities in the uppermost and lowest model layers are calculated by mass conservation. This circulation pattern is shown schematically in Fig. 1b. For the uniform upwelling velocity a typical value of 4 m yr^{-1} was used as standard for all three basins; the value is based on isotope tracer studies (e.g., Hoffert and Flannery 1985). The downwelling velocity in the northern Atlantic Ocean, representing the production of North Atlantic Deep Water (NADW), was obtained by assuming a production rate of 20 Sv (Sv $\equiv 10^6$ m^3 s^{-1}), which is consistent with estimates made by Gordon (1986). The thermohaline circulation was closed by downwelling in the Southern Ocean resulting in a production rate of 16.6 Sv of Antarctic Bottom Water (AABW).

Because the ocean model is forced by anomalies of observed sea surface temperatures (see section 3), the ocean temperature field is divided into a zonally averaged initial temperature field and a small superposed temperature perturbation field. The initial temperature field is assumed to be in thermal equilibrium and constant in time. The temperature perturbation field accounts for the propagation of the surface forcing throughout the ocean. Ocean heat mixing is strongly affected by mesoscale motions, which are not resolved by the model. A classic method of dealing with this problem is to parameterize the ocean heat mixing by diffusion. The perturbation temperature field is then affected by advection and diffusion both horizontally and vertically and can be calculated from

$$\frac{\partial T}{\partial t} + \frac{1}{Rf\cos\varphi}\frac{\partial(\cos\varphi u f T)}{\partial\varphi} + \frac{\partial(wT)}{\partial z} = \frac{1}{R^2 f\cos\varphi}\frac{\partial}{\partial\varphi}\left(f\cos\varphi K_H\frac{\partial T}{\partial\varphi}\right) + \frac{\partial}{\partial z}\left(K_V\frac{\partial T}{\partial z}\right), \quad (1)$$

where T is the perturbation temperature, R is the earth's radius, f is the fractional ocean width for each basin separately ($f_{atl} + f_{pac} + f_{ind} = 1 - f_{land}$), φ is the latitude, u is the meridional velocity, w is the vertical velocity, z is the vertical coordinate, K_H is the horizontal diffusion coefficient, and K_V is the vertical diffusion coefficient.

However, there are large uncertainties about this parameterization and especially about the magnitude of the diffusion coefficient. In simple upwelling–diffusion models, K_V is often taken to be 0.634 cm^2 s^{-1} (e.g., Warrick and Oerlemans 1990). Assuming an upwelling rate of 4 m yr^{-1}, the scale depth amounts to 500 m, which seems quite reasonable in view of observations of vertical temperature profiles (Hoffert et al. 1980). Wigley and Raper (1993) used the slightly higher value of 1.0 cm^2 s^{-1} as standard for the vertical diffusion coefficient. This constant value was also adopted in the National Center for Atmospheric Research GCM by Washington and Meehl (1989). But in the well-known GFDL (Geophysical Fluid Dynamics Laboratory) model, a vertical diffusion coefficient that varied with depth was used for several years (Bryan and Lewis 1979), whereas the diffusion in the Hamburg GCM was of a more numerical nature (Maier-Reimer et al. 1993). In tracer studies too, different values can be found for the diffusion coefficient. An interesting tracer study was performed by Gargett (1984), who argued that the diffusion coefficient should depend on the vertical stability of the water column. She therefore suggested that the diffusion coefficient should vary in inverse proportion to the Brunt–Väisälä frequency. However, others like Redi (1982) take the view that mesoscale ocean mixing occurs mainly along isopycnal surfaces. In her opinion, the orientation of the parameterized mixing should be calculated from the local slope of these surfaces.

To examine the effect that different parameterizations of the ocean heat mixing have on thermal expansion, three parameterizations are used in this study. In the first case, the ocean heat mixing is parameterized by a constant horizontal and vertical diffusion coefficient. For the horizontal diffusivity, K_H is taken equal to 4.75×10^6 cm^2 s^{-1}. This value is consistent with values usually chosen in two-dimensional ocean models (e.g., Watts and Morantine 1990; Stocker et al. 1992). For the vertical diffusivity, K_V is taken equal to 1.0 cm^2 s^{-1}, but some sensitivity experiments concerning this value will be presented. In the second case the vertical diffusivity depends on the vertical stability of the water column, as suggested by Gargett (1984). In this parameterization, $K_V = \alpha N^{-1}$ and N is the Brunt–Väisälä frequency $\{N \equiv [-g(\rho_0)^{-1}(\partial\rho/\partial z)]^{1/2}\}$. Although Gargett estimated α to be equal to 1.0×10^{-3} cm^2 s^{-1}, in this paper α is taken equal to 3.6×10^{-3} cm^2 s^{-1} after Kraus (1990). Because the largest vertical variations in the density field are generally found in the upper part of the ocean, this parameterization implies an increasing diffusion coefficient with depth. Again K_h is taken equal to 4.75×10^6 cm^2 s^{-1}. In the last case, the idea of isopycnal diffusion is tested using a technique introduced by Redi (1982). First, the local slope of the isopycnal surface in the ocean is determined and then a mixing tensor is introduced that conducts the diffusion in that direction. This technique is also used now in the GFDL model (Manabe et al. 1991). Constant values are chosen for the isopycnal

and diapycnal diffusion coefficients (1.0×10^7 cm^2 s^{-1} and 1.0 cm^2 s^{-1}, respectively).

To estimate thermal expansion in the past, one should use an initial temperature field that represents the past state of the oceans. Because the past state is unknown, an initial temperature field is used that is based on the present-day Levitus (1982) dataset. Since the ocean temperature fields toward the end of the nineteenth century were probably lower than today, an experiment was performed in which the initial ocean temperatures were reduced by one degree. The model results were affected only negligibly by this cooling. The Levitus dataset is also used to prescribe the ocean salinity fields. Then the thermal expansion of sea water, caused by changes in the perturbation temperature fields of the oceans, can be calculated using the equation of state given in Gill (1982, 600). The global mean thermal expansion is obtained by area weighting of the zonally averaged values.

3. Ocean forcing

Of course it would be useful if we could calculate thermal expansion over the last hundred years from observed changes in the three-dimensional ocean temperature and salinity fields. Unfortunately, however, this is not possible because no data exist for several ocean areas during large parts of this period. Therefore, most estimates of past thermal expansion have been obtained by the use of energy-balance climate models. Since the climate of the earth is affected by changes in radiative forcing, estimates of past climate forcing can be made from observed concentrations of greenhouse gases. Although the relationships between concentrations of greenhouse gases and radiative forcing have been fairly well established (e.g., Shine et al. 1990), there are large uncertainties in the relationships between changes in radiative forcing and temperature changes. These uncertainties are due to complex interactions and (possible) feedbacks between the different components of the climate system. In simple energy-balance climate models these uncertainties are reflected by a feedback parameter, which is specified by the change in the equilibrium global mean temperature (ΔT_{2x}) due to a doubling of the CO_2 concentration. This feedback parameter is thereby estimated to range from 1.5° to 4.5°C. The global mean surface temperature warming since the late nineteenth century is estimated to be 0.45°C (Folland et al. 1992), although considerable uncertainties remain. Model-calculated radiative forcing derived from observed concentrations of greenhouse gases can therefore be adjusted so that the simulated past global mean temperature change reflects the observations (e.g., Wigley and Raper 1993). Past thermal expansion can then be calculated from the associated changes in the ocean temperature profiles.

We used another approach. Since our attention is focused on the ocean only, it seems a good idea to take observed surface temperatures as a starting point to create ocean forcing, instead of observed concentrations of greenhouse gases. The ocean forcing in this study is derived from anomalies in observed sea surface temperatures (SST). Following the most direct way, model SST perturbations are simply equated with observed SST anomalies. The inducement to use this forcing method is the lack of knowledge of past surface heat fluxes. Estimations of these fluxes from observed concentrations of greenhouse gases, as is done in most previous studies, are based on the assumption that the enhanced greenhouse effect was the sole forcing mechanism present. Obviously, these estimated surface heat fluxes do not show the interannual variability that is observed in the SST data. By equating model SST perturbations with observed SST anomalies, the possible influence of these short-term climate fluctuations can be investigated. If the surface heat fluxes were known exactly and if a climate model would exist that calculates changes in SST due to changes in the surface heat flux perfectly, then model-calculated changes in SST would resemble exactly the observations.

The deep sea temperatures are linked to the mixed-layer temperatures by the advection–diffusion equation (1). So, in principle, the effective forcing of the deep sea in the present study is the same compared to the increased surface heat flux method used in most previous studies. However, the two forcing methods differ in practice because of the lack of knowledge of the surface heat fluxes and because of the lack of (and errors in) observations of SST. Consequently, the choice of the forcing method affects the model SST directly and the deep sea temperatures indirectly by way of the advection–diffusion equation. The differences in the temperature distributions in the ocean interior obtained with the two types of forcing will reflect the uncertainties in our observational and theoretical knowledge of the (past) climate, but will not reflect physically different forcing methods. The forcing method used in this study is therefore a reasonable and interesting tool for estimating thermal expansion in the past and for comparing these estimates with results of previous studies. Furthermore, the effects on global expansion of a regional varying ocean forcing can easily be examined by use of observed SST.

The idea of using observed surface temperatures was adopted by Church et al. (1991). However, they forced their ocean model by a global mean temperature increase that was based on both land and ocean data. Jones et al. (1986) compared records over land and over oceans for 15 regions in which land and marine observations were made in close proximity. Although their results showed good agreement for the period after 1946, there were considerable differences in their earlier records of sea surface and surface air temperatures. These discrepancies are generally thought to be caused, at least partly, by systematic errors in sea surface temperature measurements. The change from un-

insulated bucket measurements to a mixture of insulated bucket and engine intake measurements around World War II seems to be the most important reason for these errors.

Since ocean data are now readily available, only sea surface temperatures are used in this paper. Two well-known marine datasets are the Comprehensive Ocean–Atmosphere Data Set (COADS) (Woodruff et al. 1987) and the United Kingdom Meteorological Office (UKMO) dataset (Bottomley et al. 1990). The latter contains observations of sea surface temperatures and nighttime marine air temperatures, whereas COADS contains the complete set of shipboard observations. Jones et al. (1991) compared these two datasets and found important differences in the analyses of the data for the period prior to 1940. These differences are caused largely by various adjustments that were made to correct for changing methods of measuring SST, changes to ships, and changes to shipping routes. Furthermore, different grid and time intervals were used in the analyses. Here a new UKMO analysis is used, in which the COADS was used to fill in missing values in the Bottomley et al. dataset. In this analysis, improved instrumental corrections were applied concerning the wooden and canvas bucket measurements (Parker et al. 1994). This new UKMO dataset was updated to 1991; its data coverage exceeds that of the COADS. Comparisons between the new UKMO analysis and the data considered by Jones et al. (1991) were presented by Folland et al. (1992).

The UKMO dataset used in this study provides monthly mean anomalies of SST on a 5° × 5° grid for the period 1856–1991. Due to the lack of observations, not all anomaly series were complete. Some anomaly values for the northern and southern high latitudes are missing, particularly during the first half of this period. The spatial coverage is also incomplete around World War II. However, the dataset also provides seasonal SST anomalies for several regions, including the North and South Atlantic, Pacific, and Indian Oceans. Moreover, global and hemispheric mean seasonal SST anomalies are presented. All these seasonal anomaly series are complete. Three different ocean forcing types were derived for this spatial and temporal coverage of the dataset. The first is based on the complete time series of global mean seasonal SST anomalies and is called "global forcing." The second forcing type is obtained from six seasonal SST anomalies, connected with the Northern or Southern Hemispheric part of each ocean. This forcing type is called "regional forcing." The third ocean forcing type is based on the monthly mean SST anomalies for each 5° × 5° field. Because the ocean model used in this study consists of three zonally averaged ocean basins, zonal mean anomalies are calculated from these 5° × 5° values for each ocean basin. To deal with the incompleteness of some anomaly series, we combined anomaly values for the most northern and southern parts of each ocean. This means that for the Atlantic Ocean anomaly values north of 55°N are combined into a single anomaly series, so are anomaly values south of 35°S. For the Pacific Ocean these limits are 45°N and 35°S, and for the Indian Ocean, 10°N and 35°S. Therefore, inaccuracies in sea level rise caused by thermal expansion, which are introduced by this forcing method, are probably largest for the high-latitude areas. However, because the high-latitude ocean areas are small compared to the total ocean area and because the expansion coefficient is much less in colder waters, these inaccuracies will hardly affect the global mean sea level rise. Because this third ocean forcing type has a more two-dimensional nature, it is called "2D forcing."

The SST anomalies provided by the UKMO dataset are based on observations for the 1951–1980 period. This period was chosen because of the relatively good coverage with regard to the observations. Figure 2 shows these global mean seasonal SST anomalies for the entire period 1856–1991 and the 5-yr running mean values. These smoothed averages show fluctuations, with a dip of about 0.3°C in the beginning of the twentieth century, followed by a gradual rise of over 0.4°C over 30 yr; then there is another 30-yr period of little long-term change followed by another rise toward the end of the twentieth century. The average values for the Pacific Ocean (not shown) look similar to the global means, but the curve of these values for the Atlantic Ocean shows a somewhat steeper rise after the dip at the beginning of the twentieth century, whereas the average curve for the Indian Ocean shows a somewhat steeper rise toward the end of the twentieth century. Because model SST perturbations are equated here with observed SST anomalies, all these anomalies have to be offset in order to have the first years of the simulation as the zero-mean reference period. So starting the simulation in 1856 and using the same 30-yr reference period as Bottomley et al. (1990), we have to use the offset SST anomalies based on observations for the period 1856–1885. Since the data coverage during this period is poor and the emphasis of this study is on thermal expansion over the past hundred years, most simulations presented here start in 1891 and have 1891–1920 as the zero-mean reference period.

4. Experiments

a. Global and regional forcing

In the first experiment, model SST perturbations were equated with the global mean seasonal SST anomalies, as shown in Fig. 2. The propagation of this ocean surface forcing throughout the deep ocean during the period 1891–1991 was determined by the advection–diffusion equation (1), using a constant vertical diffusion coefficient of $K_V = 1.0\ \text{cm}^2\ \text{s}^{-1}$. The resulting temperature changes were used to calculate changes in the density field. On the assumption that the ocean grid-

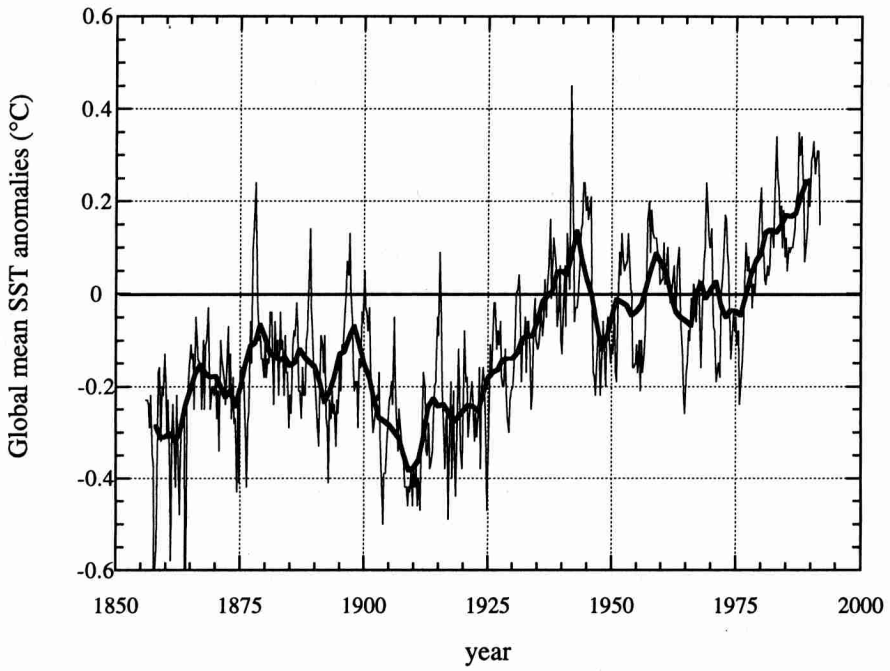

FIG. 2. Global mean seasonal SST anomalies and the running mean values for 5 yr. The period 1951–1980 is the reference period.

box volumes remain constant, these local density variations are translated into local sea level variations. In Fig. 3a these values are shown for each separate ocean basin. The local sea level variations in the high northern Atlantic Ocean are remarkably large. In this part of the Atlantic Ocean basin the downwelling represents the formation of NADW. So in this ocean area, perturbations of the sea surface temperature are transported downward both by diffusion and by advection, leading to relatively large values of local thermal expansion. However, this local thermal expansion has only a minor effect on the global mean sea level rise because of the small surface area involved. In the northern Pacific Ocean, considerably smaller local expansion rates are found because of the absence of downwelling there. Moreover, the initial temperature field affects the thermal expansion: since the Atlantic Ocean is warmer than the Pacific Ocean north of 20°N in the present state, the high expansion rates due to the downwelling effect are intensified by the larger thermal expansion coefficients in the northern Atlantic Ocean. In the Pacific and Indian Oceans, in which there is only upwelling, the general trend is that local contributions are highest near the equator. The higher ocean temperatures in this area cause larger thermal expansion coefficients.

The amounts of local thermal expansion in each ocean basin at the end of the simulation are combined by area weighting to obtain zonally averaged values for one fictitious global ocean. These values are shown in Fig. 3b for the global forcing type considered above, as well as for the other two forcing types. The zonal mean values in the high northern latitudes are remarkably large for all three ocean forcing types. However, this is misleading to a certain extent since the northernmost latitudes of the fictitious global ocean consist only of the part of the Atlantic Ocean basin that is representative of downwelling NADW. As mentioned before, these local Atlantic contributions have only a minor affect on global mean sea level rise because of the small surface area involved.

The results for the three ocean forcing types bear a strong resemblance. As the trends in the observed SST anomalies are somewhat more pronounced in the high latitudes, especially in the northern Atlantic Ocean, the largest amounts of thermal expansion in the Northern Hemisphere are found for the 2D forcing type. Using the other two forcing types, this trend is spread more evenly, leading to higher rates of thermal expansion near the equator. Irregularities in the results for the 2D forcing type are caused by the two-dimensional nature of the surface ocean forcing. By area weighting of the zonally averaged values we can estimate the global mean sea level rise due to thermal expansion during the selected period. Since about 60% of the oceans are situated in the Southern Hemisphere, this global mean value is hardly affected by the different forcing types. Model-calculated values are 3.37, 3.44, and 3.47 cm for global, regional, and 2D forcing, respectively.

b. Start of the simulations

In the previous experiment the simulations started in 1891 and the observed SST anomalies were offset so

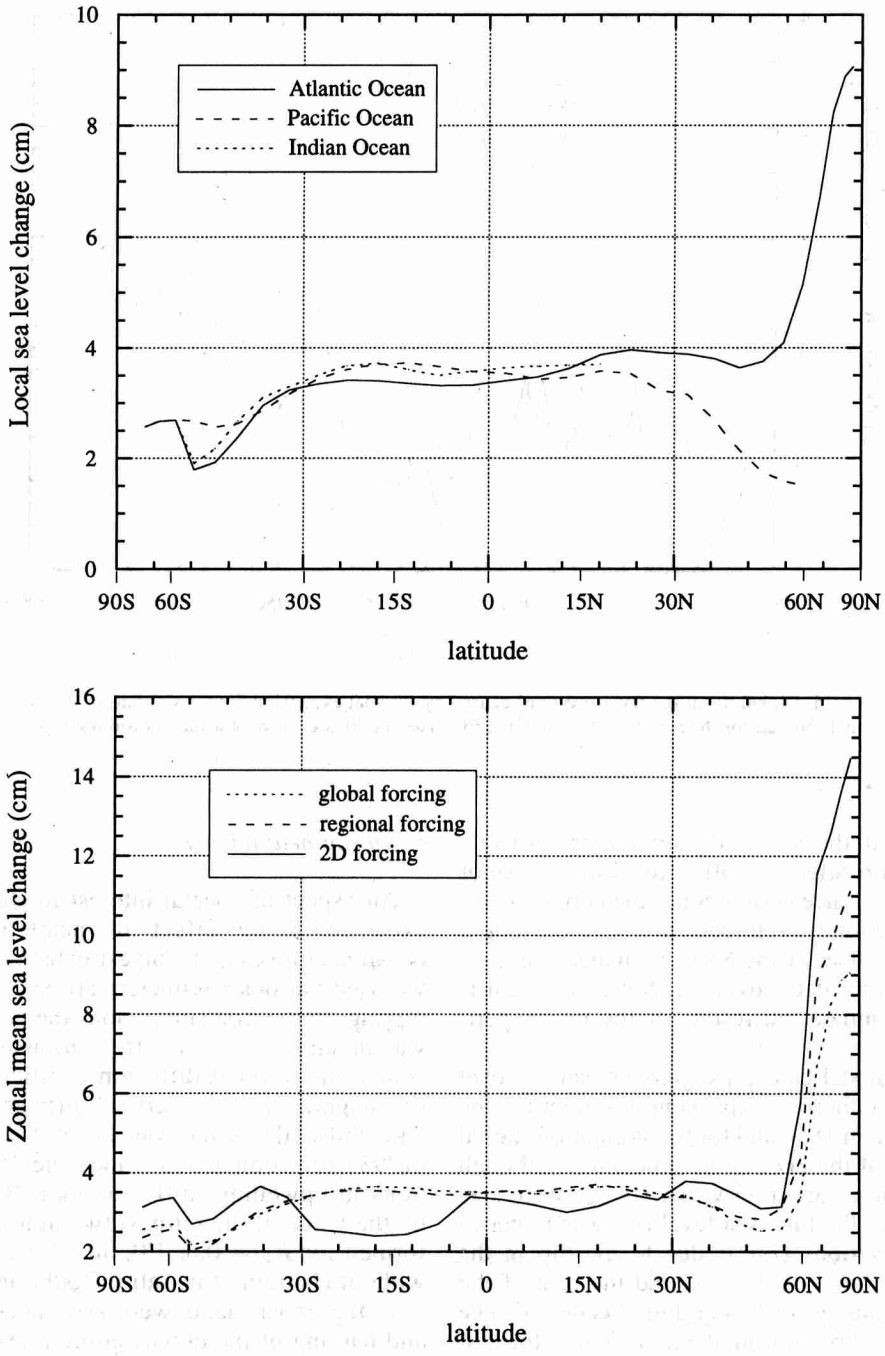

FIG. 3. (a) Latitudinal variation in the local contributions (cm) of all three oceans to the global mean sea level rise caused by thermal expansion during the period 1891–1991. The results are obtained by use of the 2D forcing type. (b) Meridional distribution of the zonal mean contributions (cm) of all oceans together to the global mean sea level rise caused by thermal expansion during the period 1891–1991. Results are shown for the global, regional, and 2D forcing types. Note that sine(latitude) is used as the absissca to reflect area weighting.

that we could have 1891–1920 as our zero-mean reference period. Since the dataset contains anomalies from 1856, the simulations of thermal expansion in the past were repeated with this year as the starting point. Again, the present-day Levitus (1982) dataset was used to prescribe the initial ocean temperature and salinity fields. We performed this longer simulation in order to get insight into the possible effects of a previous warm-

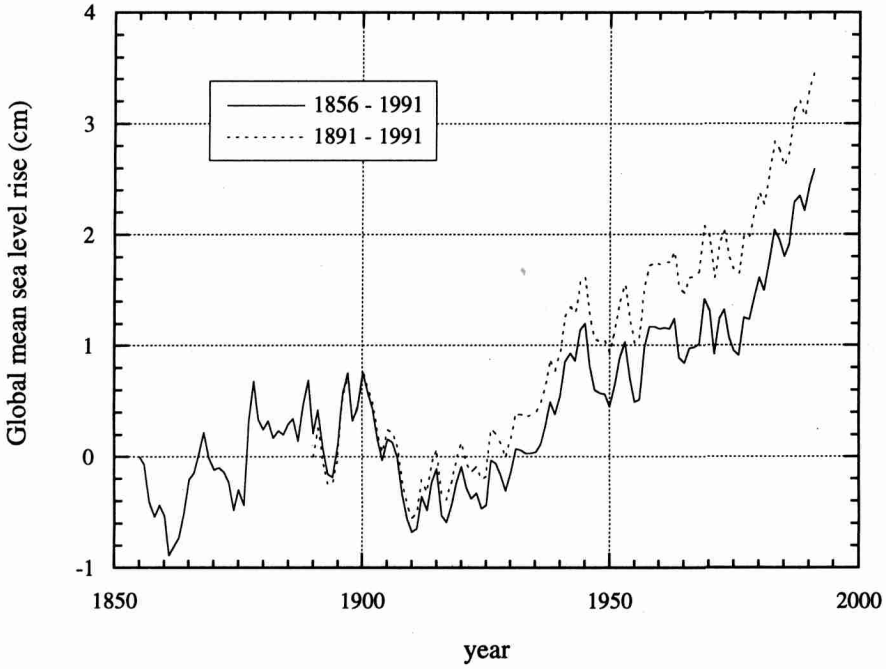

FIG. 4. Global mean sea level rise (cm) caused by thermal expansion for the simulation started in 1856 and for the simulation started in 1891. The results are shown for the 2D forcing type.

ing history prior to the start of the simulations in 1891. However, model results were affected by the choice of the zero-mean reference period. Since the period 1856–1885 was the zero-mean reference period in the longer simulations, the offset of the SST anomalies was then based on an inferior data coverage. Nevertheless, it is interesting to compare the results of the two experiments.

In Fig. 4, the model-calculated global mean sea level change caused by thermal expansion is shown for the simulation started in 1856 and for the simulation started in 1891, in case of the 2D forcing type only. Although the first simulation started 35 yr earlier, we were surprised to find that the final sea level rise was larger in the second simulation. This is due to the dip in the observed SST anomaly values around the turn of the century, which cause a sea level fall in this period. The calculated sea level rise during the first 35 yr in the first simulation is largely offset by this sea level fall, whereas in the second simulation this dip is mainly enclosed in the zero-mean reference period. However, after the turn of the century differences in offset values cause higher temperature anomalies in the second simulation, leading to larger thermal expansion rates. Differences in thermal expansion between the three forcing types are more pronounced in the longer simulations. Model-calculated values for the global mean sea level rise for the simulations started in 1856 are 2.96, 3.00, and 2.59 cm for global, regional, and 2D forcing, respectively.

c. *Ocean heat mixing*

An aspect of special interest in studies of thermal expansion is the effect of uncertainties in vertical ocean heat mixing. To investigate these uncertainties, we used various parameterizations of the ocean heat mixing. In the first simulations the ocean heat mixing was parameterized by diffusion, using uniform horizontal and vertical diffusion coefficients. We varied the magnitude of the vertical diffusion coefficient K_V and chose the same values as Wigley and Raper (1993) for comparison. Since the steady-state solutions in upwelling–diffusion models are determined by the value of the ratio K_V/w, simulations were performed for $K_V = 0.5$, 1.0, and 2.0 cm^2 s^{-1} with and without changing this ratio. Doubling and halving of w in the experiments were associated with doubling and halving of the downwelling rates of NADW and AABW for mass conservation reasons. As for a certain value of the vertical diffusion coefficient, the results were most pronounced for a constant ratio K_V/w, only results are shown for experiments in which this ratio remained the same.

In addition, a simulation was performed in which the vertical diffusivity was assumed to depend on the vertical stability of the water column. In this simulation $K_V = \alpha N^{-1}$, with N is the Brunt–Väisälä frequency and $\alpha = 3.6 \times 10^{-3}$ cm^2 s^{-1}. If the water column was unstably stratified, $K_V = 1.0 \times 10^2$ cm^2 s^{-1} was used. In a third simulation, the concept of isopycnal diffusion

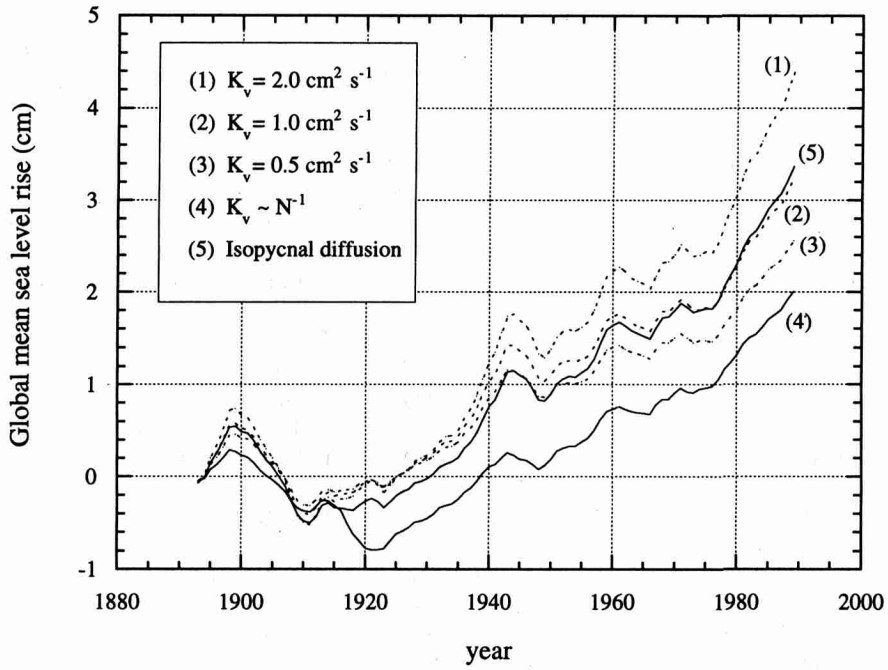

FIG. 5. Global mean sea level variation (cm) caused by thermal expansion during the period 1891–1991. The results are shown for the 2D forcing type. Ocean heat mixing is parameterized by constant vertical diffusion coefficients (1–3, dotted lines), by a stability-dependent vertical diffusion coefficient (4, solid line), and by isopycnal diffusion (5, solid line).

was tested using a constant diapycnal and isopycnal diffusion coefficient (1.0 cm^2 s^{-1} and 1.0 × 10^7 cm^2 s^{-1}, respectively).

In Fig. 5, we present the resulting estimates of the global mean sea level rise caused by thermal expansion during the period 1891–1991 as 5-yr running means for the 2D forcing type only. During the first part of the simulation, thermal expansion is hardly affected by the different parameterizations of the ocean heat mixing. Thereafter, however, the choice of the parameterization does affect the thermal expansion. Using a uniform vertical diffusion coefficient, the downward heat transport is faster for larger diffusion coefficients and the warming of the deeper ocean layers is larger, which thereby contributes more to thermal expansion. Final values for the global mean sea level rise obtained in this experiment for a constant ratio K_V/w are 2.48, 3.47, and 5.14 cm for K_V = 0.5, 1.0, and 2.0 cm^2 s^{-1}, respectively. These values are very similar to those given by Wigley and Raper, but slightly smaller. However, if the vertical diffusivity is assumed to depend on the vertical stability of the water column, the model calculates a larger sea level fall at the beginning of the twentieth century, due to the dip in the observed SST anomalies. Because this dip reduced the stability of the upper part of the water column, larger vertical diffusion coefficients were determined during this period, which caused a faster downward transport of the negative SST perturbation. Because of this larger sea level fall, the final sea level rise is smaller than for the K_V = 0.5 cm^2 s^{-1} simulation (viz. 2.18 cm for the 2D forcing type). If the isopycnal diffusion method is used, model-calculated global mean sea level rise is smaller than for a constant vertical diffusion coefficient until about 1950. Thereafter the sea level seems to rise faster. The final global mean sea level rise (3.63 cm for the 2D forcing type) is almost the same as for the K_V = 1.0 cm^2 s^{-1} simulation.

The physical processes responsible for mixing in the interior of the oceans are poorly understood. To parameterize the ocean mixing by diffusion, assumptions have to be made concerning the magnitude of the diffusion coefficients and the orientation of the diffusion. All the parameterizations of the ocean heat mixing used in this study seem to be reasonable and it is difficult to prefer one rather than the other. The variations in the model results obtained for various parameterizations should therefore be considered to reflect the existing uncertainties in ocean heat mixing. These uncertainties are of the same order as those introduced by the choice of the starting point of the simulations. However, the longer simulations have the major disadvantage of a poor data coverage in the beginning of the simulation period. Therefore, in this study, global mean sea level rise caused by thermal expansion over the past hundred years is estimated to be in the range of 2.2–5.1 cm, a best estimate being 3.5 cm. In spite of the fact that we used a more sophisticated model in this study and a

different approach to force the ocean model, the values found for thermal expansion differ only slightly from previous estimates.

5. Conclusions

Estimates of sea level rise due to thermal expansion during the period 1856–1991 have been presented. Our study differs from most previous studies in that we used a zonally averaged ocean model, in which the ocean circulation is prescribed. The model consists of three ocean basins, representing the Atlantic, Pacific, and Indian Oceans, which are connected by a circumpolar basin that represents the Southern Ocean. The ocean surface forcing was based on observed sea surface temperatures instead of radiative forcing. Experiments were done with three forcing types, which are of a global, a regional, and a more two-dimensional nature. In the model, only ocean temperature perturbations were considered since the initial temperature field was assumed to be in thermal equilibrium. Because the ocean temperatures at the beginning of the selected period are unknown, the present-day temperatures were chosen as the initial temperature distribution.

Mainly due to downwelling in the northern Atlantic Ocean, which represents the production of North Atlantic Deep Water, local thermal expansion in the northern Atlantic Ocean is considerably larger than in the northern Pacific Ocean. Furthermore, model calculations indicate that local thermal expansion is somewhat higher in the Northern Hemisphere in case of the 2D forcing than in case of the global forcing. Results in terms of global mean sea level rise differ only slightly. Model results are also affected by the choice of the starting point of the simulations. If the calculations are started in 1856, thermal expansion rates are found to be lower than if the calculations are started in 1891. However, the data coverage toward the end of the nineteenth century is poor, so that expansion rates in the longer simulations are uncertain.

Different parameterizations of the ocean heat mixing were also considered in this study, namely diffusion by use of uniform diffusion coefficients, diffusion in which the vertical diffusivity was assumed to depend on the vertical stability of the water column, and isopycnal diffusion. Because all these parameterizations seem to be reasonable, differences in the model results are considered to reflect the existing uncertainties concerning ocean mixing. In this study, global mean sea level rise caused by thermal expansion over the past hundred years is estimated to be in the range 2.2–5.1 cm, a best estimate being 3.5 cm. These values are smaller than the values estimated by Church et al. (1991), who also used observed temperatures to force their (three-dimensional) ocean model. Part of the difference may be explained by the fact that they used observed global mean surface air temperatures, whereas we used observed zonal mean sea surface temperatures.

Values found for thermal expansion in this study are in close agreement with previous estimates obtained by means of simpler one-dimensional upwelling–diffusion models. This agreement is due to the fact that such a model represents the equatorial and midlatitudinal ocean areas reasonably. On the other hand, we found relatively large rates of local thermal expansion in the high-latitude downwelling areas, which are not represented in one-dimensional models. These local values have only a minor effect on the global mean sea level rise because of the small ocean areas on high-latitudes. In spite of the slight differences in global mean sea level rise obtained by means of our model and by means of simpler one-dimensional models, it is useful to estimate thermal expansion by means of the more sophisticated model. An advantage of our model compared with one-dimensional models is the more realistic representation of the ocean thermohaline circulation. The ratio of the polar-sinking water temperature change to the global mean temperature change is determined in our model by the integration of the advection–diffusion equation, whereas this ratio has to be prescribed in the one-dimensional models. Furthermore, to estimate thermal expansion in the future, an atmospheric energy-balance model can be coupled easily to our ocean model, together with a sea ice model. By means of such a climate model, one can examine the effect of several climate aspects on thermal expansion, which require some horizontal resolution such as the albedo–temperature feedback and possible changes in the sea ice coverage. However, a disadvantage of all upwelling–diffusion models compared with GCMs is the extremely simple representation of processes involved in the penetration and distribution of heat from the surface to the interior of the ocean. Since these simplifications make the upwelling–diffusion models cheap in computer time, they still are useful to perform a wide range of sensitivity experiments.

Acknowledgments. Financial support for this work was obtained from Rijkswaterstaat, RIKZ (project "ZEESPIEG").

REFERENCES

Barnett, T. P., 1985: Long-term climate change in observed physical properties of the oceans. *Detecting the Climatic Effects of Increasing Carbon Dioxide*, M. C. MacCracken and F. M. Luther, Eds., US DOE/ER-0235, 91–107.

Bottomley, M., C. K. Folland, J. Hsiung, R. E. Newell, and D. E. Parker, 1990: *Global Ocean Surface Temperature Atlas*, MIT Press, 20 pp. plus 313 plates.

Bryan, K., and L. J. Lewis, 1979: A Water Mass Model of the World Ocean. *J. Geophys. Res.*, **84**, 2503–2517.

Church, J. A., J. S. Godfrey, D. R. Jackett, and T. J. McDougall, 1991: A model of sea level rise caused by ocean thermal expansion. *J. Climate*, **4**, 438–456.

Cubasch, U., K. Hasselmann, H. Höck, E. Maier-Reimer, U. Mikolajewicz, B. D. Santer, and R. Sausen, 1992: Time-dependent greenhouse warming computations with a coupled ocean–atmosphere model. *Climate Dyn.*, **8**, 55–69.

Douglas, B. C., 1991: Global sea level rise. *J. Geophys. Res.*, **96,** 6981–6992.

Folland, C. K., T. R. Karl, N. Nicholls, B. S. Nyenzi, D. E. Parker, and K. Ya. Vinnikov, 1992: Observed climate variability and change. *Climatic Change 1992. The Supplementary Report to the IPCC Scientific Assessment,* J. T. Houghton, B. A. Callander, and S. K. Varney, Eds., Cambridge University Press, 135–170.

Gargett, A. E., 1984: Vertical eddy diffusivity in the ocean interior. *J. Mar. Res.*, **42,** 359–393.

Gill, A. E., 1982: *Atmosphere–Ocean Dynamics.* Academic Press, 662 pp.

Gordon, A. L., 1986: Interocean exchange of thermocline water. *J. Geophys. Res.*, **91,** 5037–5046.

Gornitz, V., S. Lebedeff, and J. Hansen, 1982: Global sea level trends in the past century. *Science,* **215,** 1611–1614.

Gregory, J. M., 1993: Sea level changes under increasing atmospheric CO_2 in a transient coupled ocean–atmosphere GCM experiment. *J. Climate,* **6,** 2247–2262.

Hoffert, M. I., and B. P. Flannery, 1985: Model projections of the time-dependent response to increasing carbon dioxide. *Projecting the Climatic Effects of Increasing Carbon Dioxide,* M. C. MacCracken and F. M. Luther, Eds., U. S. Department of Energy, Carbon Dioxide Research Division, 149–190.

——, A. J. Callegari, and C.-T. Hsieh, 1980: The role of deep sea heat storage in the secular response to climatic forcing. *J. Geophys. Res.*, **85,** 6667–6679.

Jones, P. D., T. M. L. Wigley, and P. B. Wright, 1986: Global temperature variations between 1861 and 1984. *Nature,* **322,** 430–434.

——, ——, and G. Farmer, 1991: Marine and land temperature data sets: A comparison and a look at recent trends. *Greenhouse-Gas-Induced Climatic Change: A Critical Appraisal of Simulations and Observations,* M. E. Schlesinger, Ed., Elsevier Science, 153–172.

Kraus, E. B., 1990: Diapycnal mixing. *Climate–Ocean Interaction,* M. E. Schlesinger, Ed., Kluwer Academic, 269–293.

Levitus, S., 1982: *Climatological Atlas of the World Ocean.* NOAA Prof. Paper 13, U.S. Govt. Printing Office, Washington, DC, 177 pp.

Maier-Reimer, E., U. Mikolajewicz, and K. Hasselmann, 1993: Mean circulation of the Hamburg LSG OGCM and its sensitivity to the thermohaline surface forcing. *J. Phys. Oceanogr.*, **23,** 731–757.

Manabe, S., and R. J. Stouffer, 1994: Multiple-century response of a coupled ocean–atmosphere model to an increase of atmospheric carbon dioxide. *J. Climate,* **7,** 5–23.

——, ——, M. J. Spelman, and K. Bryan, 1991: Transient response of a coupled ocean–atmosphere model to gradual changes of atmospheric CO_2. Part I: Annual mean response. *J. Climate,* **4,** 785–818.

Mikolajewicz, U., B. D. Santer, and E. Maier-Reimer, 1990: Ocean response to greenhouse warming. *Nature,* **345,** 589–593.

Parker, D. E., P. D. Jones, C. K. Folland, and A. Bevan, 1994: Interdecadal changes of surface temperature since the late nineteenth century. *J. Geophys. Res.*, **99,** 14 373–14 399.

Redi, M. H., 1982: Oceanic isopycnal mixing by coordinate rotation. *J. Phys. Oceanogr.*, **12,** 1154–1158.

Robin, G. de Q., 1986: Changing the sea level. *The Greenhouse Effect, Climatic Change and Ecosystems,* B. Bolin, B. R. Döös, J. Jäger, and R. A. Warrick, Eds., John Wiley and Sons, 323–359.

Shine, K. P., R. G. Derwent, D. J. Wuebbles, and J.-J. Morcrette, 1990: Radiative forcing of climate. *Climatic Change: The IPCC Scientific Assessment,* J. T. Houghton, G. J. Jenkins, and J. J. Ephraums, Eds., Cambridge University Press, 41–68.

Stocker, T. F., D. G. Wright, and L. A. Mysak, 1992: A zonally averaged, coupled ocean–atmosphere model for paleoclimatic studies. *J. Climate,* **5,** 773–797.

Warrick, R. A., and J. Oerlemans, 1990: Sea level rise. *Climatic Change: The IPCC Scientific Assessment,* J. T. Houghton, G. J. Jenkins, and J. J. Ephraums, Eds., Cambridge University Press, 257–282.

Washington, W. M., and G. A. Meehl, 1989: Climate sensitivity due to increased CO_2: Experiments with a coupled atmosphere and ocean general circulation model. *Climate Dyn.*, **4,** 1–38.

Watts, R. G., and M. Morantine, 1990: Rapid climatic change and the deep ocean. *Climatic Change,* **16,** 83–97.

Wigley, T. M. L., and S. C. B. Raper, 1987: Thermal expansion of sea water associated with global warming. *Nature,* **330,** 127–131.

——, and ——, 1993: Future changes in global mean temperature and sea level. *Climate and Sea Level Change: Observations, Projections and Implications,* R. A. Warrick, E. M. Barrow, and T. M. L. Wigley, Eds., Cambridge University Press, 111–133.

Woodruff, S. D., R. J. Slutz, R. J. Jenne, and P. M. Steurer, 1987: A Comprehensive Ocean–Atmosphere Data Set. *Bull. Amer. Meteor. Soc.,* **68,** 1239–1250.

Woodworth, P. L., 1993: A review of recent sea-level research. *Oceanogr. Mar. Biol.,* **31,** 87–109.